THEORY

Fault Tolerant Control via Input-Output Linearization Method for LED-Driver Using a Boost Converter

GERARDO ORTIZ TORRES[1], (Member, IEEE), **JESSE Y. RUMBO-MORALES**[1], (Member, IEEE), **RENÉ OSORIO SÁNCHEZ**[1], **MARIO MARTÍNEZ-GARCÍA**[1], **AND MARCO ANTONIO RODRÍGUEZ BLANCO**[2]

[1]Centro Universitario de los Valles, Universidad de Guadalajara, Ameca, Jalisco 46600, Mexico
[2]Facultad de Ingeniería, Universidad Autonoma del Carmen, Campeche 24180, Mexico

Corresponding author: Mario Martínez-García (mario.mgarcia@academicos.udg.mx)

ABSTRACT This paper proposes a method based on an input-output linearization controller with a nonlinear adaptive observer, in order to achieve both an effective light-emitting diode (LED) current tracking and an actuator fault tolerant controller strategy for a LED-driver, using a boost converter. The partial fault is presented as a Loss of Effectiveness (LoE) in the embedded control target by considering that it generates a faulty Pulse-Width Modulation (PWM) signal. Also, faults of energy storage components in the power system are considered as actuator partial faults. An internal stability analysis is presented to ensure the feasibility of the nonlinear controller design. The nominal feedback controller is able to compensate for the nonlinearity of the system exactly, thus yielding a linear control loop. Furthermore, a nonlinear adaptive observer is considered for fault estimation. When the actuator fault is detected and estimated correctly, fault accommodation and reconfiguration strategies are performed to reduce the fault's effect. The controller and observer gains are tuned using genetic algorithm techniques to have a desired closed-loop and fault estimation error response. Finally, simulations results are done in order to illustrate the effectiveness of the proposed methodology.

INDEX TERMS Boost converter, fault tolerant control, genetic algorithm, input-output linearization, LED-driver.

I. INTRODUCTION

Power light-emitting diodes (LEDs) are the most efficient light source in the market and have a long useful life [1]. The power LED-driver system generally uses a power converter, like a DC-DC boost converter, to obtain a constant LED current. The boost converter as a LED-driver has been used with satisfactory results in LED lighting applications [1], [2]. This converter is a nonlinear system, also second order non-minimum phase converter, and due to this property, it is difficult to control it [3]. The boost converter system has a right-half-plane zero that can unstablilize the system dynamics in direct voltage regulation [3]. Additionally, power

The associate editor coordinating the review of this manuscript and approving it for publication was Fanbiao Li.

LEDs are sensitive to current variations; in extreme case, these variations can damage some essential component or even destroy them. Therefore, a LED-driver based on a DC-DC converter requires a trustworthy nominal controller. Furthermore, a Fault Tolerant Control (FTC) method can be considered in order to identify malfunctions at any time and to improve reliability and safety. The FTC techniques are classified into two types [4]: passive and active. In the active techniques, the controller parameters are adapted or reconfigured according to the fault using the information of the Fault Diagnosis (FD) system, so that the stability and acceptable performance of the system can be maintained.

Several controller designs have been proposed, such as [1], where an effective LED current control for a LED-driver system based on a DC-DC boost converter with a Digital

Pulse-Width Modulation (DPWM) and a Pulse-Skip Modulation (PSM) are designed. In [2], an LED-driver consisting of dimmable current regulators and a boost converter with Adaptive Reference Tracking Control (ARTC) is proposed. Experimental results demonstrate an effective LED current control with a voltage alteration compensation. A design of a fractional order PID-type controller for a boost converter is considered in [5]. The closed-loop system transfer function is approximated to a first order system with unit gain. An implementation of multi-step direct Model Predictive Control (MPC) for DC-DC boost converters is presented in [6]. The proposed controller is robust against parameter uncertainties and can decrease real-time calculations significantly, compared with other similar controllers. Also, an accurate tracking of dynamic inductor current and output voltage is obtained. Recently, [7] have proposed a nonlinear controller scheme based on input-output linearization control strategy to achieve power factor correction and output voltage constant in a AC-DC boost converter. Simulation and experimental results show that the phases of input voltage and input current are consistent, and the voltage remains constant under load step changes.

Recent works on FD and FTC design for boost converters subjected to faults can be found in [8], [9], [10], [11], [12], and [13]. In the literature, mainly two faults in a boost converter, on the power device, are considered: Open Circuit Faults (OCFs) and Short Circuit Faults (SCFs). In this context, an effective robust FD for DC-DC boost converter via switched system is presented in [8]. Capacitor and inductor partial faults are detected and estimated using the proposed method with effective experimental results. According to the previous works on DC-DC converter fault detection, the energy storage components faults in the power electronic systems are rarely considered. So, the motivation of this paper is to considers actuator partial faults presented as a Loss of Effectiveness (LoE) that can be seen as a fault in the embedded target control or as a fault in the energy storage components in the power system. Additionally, this paper presents the design of a nonlinear controller and a FTC strategy using a nonlinear adaptive observer for detection, estimation, accommodation and reconfiguration of the fault. The main contribution of this work is the design and validation of a FD and FTC schemes by using the fault estimation information in order to accommodate partial faults, presented in the energy storage components (capacitor and inductor) or presented as faulty Pulse-Width Modulation (PWM) signal for LED-Driver system using a boost converter.

This document is organized as follows: In Section II, the system modelling is presented. The nominal feedback control design is shown in Section III. Section IV presents the actuator fault tolerant control system. In order to demonstrate the effectiveness of the proposed scheme, simulation results are presented in Section V. Finally, conclusions are depicted in Section VI.

II. SYSTEM MODELING

Figure 1 shows the schematic diagram of the DC-DC converter, named as boost converter, used as a LED-driver. The boost converter uses a MOSFET transistor M, a diode D, an inductor $L = 1.48\ mH$, and a capacitor $C = 6.18\ \mu F$. The LED model designed in our previous work [14] is used to represented the LED-driver system. It consists of a constant voltage source E_y in series with a constant resistor R_y, shown in Figure 1b. The model parameters can be obtained by means of adjusting the experimental LED Voltage-Current (V-I) curve, using the following equation:

$$v_{LED} = R_y i_{LED} + E_y, \tag{1}$$

where v_{LED} and i_{LED} are the LED voltage and current, respectively. The experimental and theoretical curve for the twelve LEDs panel (LMT-P12Y-77-N from SiLed Company) are shown in Figure 2. Therefore, by using (1) and the curve from Figure 2, the adjusting results for the LED panel are $R_y = 22.54\ \Omega$ and $E_y = 32.51\ v$.
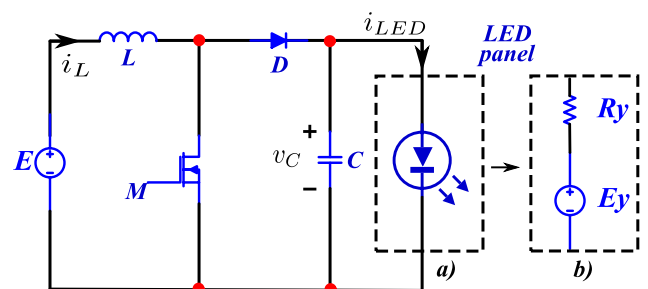

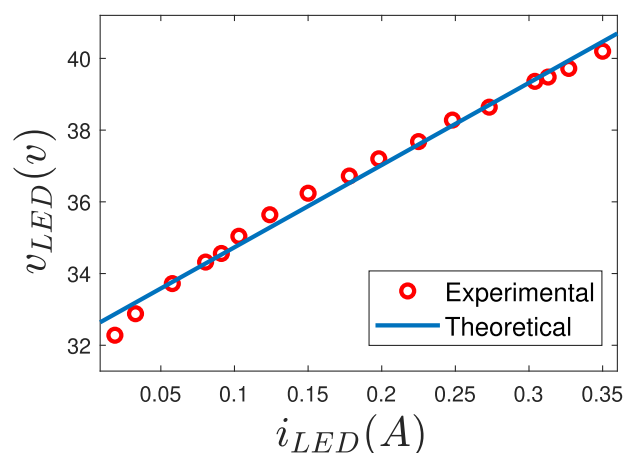**FIGURE 1.** Schematic diagram of the power stage. a) LED panel, b) LED-driver model.

FIGURE 2. Experimental and theoretical curve of the twelve LEDs panel.

An average differential equations of the DC-DC converter is calculated to obtain a simpler model for control design purposes. The MOSFET transistor M can be seen as an active controllable switch. Thus, the following approximate

averaged nonlinear model is obtained:

$$\dot{i}_L = -\frac{1}{L}v_C(1-u) + \frac{1}{L}E, \tag{2}$$

$$\dot{v}_C = \frac{1}{C}i_L(1-u) - \frac{1}{CR_y}v_C + \frac{1}{CR_y}E_y, \tag{3}$$

where i_L, v_C and u are the inductor current, the capacitor voltage and the control input, respectively. The control input u is generated via a Pulse-Width Modulation (PWM) with a duty-cycle from 0 to 1. A relation between inductor current i_L and capacitor voltage v_c can be obtained in steady-state conditions, by considering $v_c \geq E > 0$ with the steady-state input $u_{ss} = 1 - E/v_c$. Then, from (3), the following relation is stated:

$$i_L = \frac{v_c^2 - v_cE_y}{ER_y}. \tag{4}$$

III. NOMINAL NONLINEAR CONTROLLER DESIGN

The objective is to apply the input-output linearization strategy in order to design a nominal controller for the nonlinear system (2) and (3). The designed nonlinear feedback controller will be able to compensate the nonlinearity of the system exactly thus yielding a linear control loop. Then, a linear controller is designed for tracking the LED current i_{LED} by using the proposed nonlinear transformation. The nonlinear system (2) and (3) can be rewritten in the single-input single-output affine system form, as follows:

$$\dot{x} = f(x) + g(x)u, \qquad y = h(x), \tag{5}$$

with

$$f(x) = \begin{bmatrix} -\frac{1}{L}x_2 + \frac{1}{L}E \\ -\frac{1}{CR_y}x_2 + \frac{1}{C}x_1 + \frac{1}{CR_y}E_y \end{bmatrix},$$

$$g(x) = \begin{bmatrix} \frac{1}{L}x_2 \\ -\frac{1}{C}x_1 \end{bmatrix},$$

where $x = [i_L, v_c]^\top = [x_1, x_2]^\top \in \mathbb{R}^n$ is the state vector, $u \in \mathbb{R}^m$ is the manipulated input, $y \in \mathbb{R}^m$ is the output and $f(x) \in \mathbb{R}^n$, $g(x) \in \mathbb{R}^{n \times m}$ and $h(x) \in \mathbb{R}^m$ are nonlinear functions of the states. In this paper, the term E_y/CR_y in (3) is not considered in the controller design because it lead to an unfeasible input-output linearization with unstable zero dynamics [15], nevertheless it will be compensated by the control law. The proposed output variable $y = h(x)$ will be discussed below.

The derivative of the output y is described by:

$$\dot{y} = \frac{\partial h(x)}{\partial x}f(x) + \frac{\partial h(x)}{\partial x}g(x)u$$
$$= L_f h(x) + L_g h(x)u, \tag{6}$$

where $L_f h$ and $L_g h$ are called the Lie derivative of $h(x)$ with respect of $f(x)$ and $g(x)$, respectively. The output y needs to be differentiated for r times until it is directly related to the input u. The integer r is called relative degree of the system (5) and it exists at a point x_0 if the following conditions are satisfied: i) $L_g L_f^k h(x) = 0$ $\forall x$ in a neighborhood of x_0 and

all $k < r - 1$, and ii) $L_g L_f^{r-1}h(x) \neq 0$. In other words, if both conditions holds it means that u does not appear in the equations of $y, \dot{y}, \ldots, y^{r-1}$ and appears in y^r with a nonzero coefficient, as:

$$y^r = L_f^r h(x) + L_g L_f^{r-1}h(x)u. \tag{7}$$

Then, by using (7), the state feedback control law is represented by:

$$u = \frac{-L_f^r h(x) + v}{L_g L_f^{r-1} h(x)}. \tag{8}$$

From (8) is clear that the system (5) is input-output linearizable because of the input-output map $y^r = u$. The map between the new input v and the output y is exactly linear for all x in the neighborhood of x_0. Then, a nonlinear transformation of a coordinate in state-space, called local diffeomorphism, is achieved as $z = \Phi(x)$. If the output function $h(x)$ makes relative degree r of the system equal to the system order n ($r = n$), then the nonlinear system (5) can be completely linearized under a new coordinate system; otherwise, if the output function $h(x)$ makes $r < n$, called as internal dynamics, then the closed-loop nonlinear system can be only partially linearized and includes a linear and a nonliner component. If the output $y = 0$ in the internal dynamics, then it is defined as zero dynamics [15]. If the zero dynamics is stable, the nonlinear system (5) is a minimum phase system and it is possible to design the input-output linearization strategy. Moreover, if the zero dynamics is unstable, the system is non-minimum phase and the linearization controller design is unfeasible. In this case a new output function $h(x)$ has to be proposed to ensure zero dynamics stability.

Note that by selecting $h(x) = x_1 = i_L$ or $h(x) = x_2 = v_c$, the relative degree of the system (5) is $r = 1 < n$, with $n = 2$. Thus, the internal dynamics needs to be analyzed in order to select an appropriate output function. The apparent easy way to control the LED current i_{LED} is by selecting the output function $h(x) = v_c$. However, using this output variable the controller design is unfeasible because the zero dynamics is unstable [16]. Otherwise, $h(x) = i_L$ is an appropriated output with a stable zero dynamics. The internal stability analysis with $h(x) = i_L$ is presented in the following section.

1) INTERNAL STABILITY ANALYSIS

Let consider the nonlinear system (5) with $y = h(x) = x_1$. Then, by using (6) the derivative of y with respect to time is:

$$\dot{y} = L_f h(x) + L_g h(x)u$$
$$= -\frac{1}{L}x_2 + \frac{1}{L}E + \frac{1}{L}x_2 u, \tag{9}$$

with

$$L_f h(x) = -\frac{1}{L}x_2 + \frac{1}{L}E, \qquad L_g h(x) = \frac{1}{L}x_2.$$

From (9) is clear that the relative degree of the system is $r = 1 \neq 2$ because it is differentiated one time until control

input u appear. The coordinate transformation is achieved by choosing a new state variable $\psi(x)$ according to the following condition:

$$
\begin{aligned}
L_g \psi(x) &= 0 \\
&= \frac{\partial \psi(x)}{\partial x} g(x) \\
&= \frac{\partial \psi(x)}{\partial x_1} \frac{1}{L} x_2 - \frac{\partial \psi(x)}{\partial x_2} \frac{1}{C} x_1 = 0.
\end{aligned}
\tag{10}
$$

One possible solution of (10) is $\psi(x) = \frac{1}{C} x_1^2 + \frac{1}{L} x_2^2$. Then, the new state vector $\Phi(x) = [\xi(x), \psi(x)]^\top$ is stated as follows:

$$
\xi(x) = x_1, \qquad \psi(x) = \frac{1}{C} x_1^2 + \frac{1}{L} x_2^2,
\tag{11}
$$

with the internal dynamics $\dot{\psi}(x) = \eta\big(\xi(x), \psi(x)\big)$ defined as:

$$
\begin{aligned}
\dot{\psi}(x) &= \frac{2}{C} x_1 \dot{x}_1 + \frac{2}{L} x_2 \dot{x}_2 = \frac{2E}{LC} x_1 - \frac{2}{LCR_y} x_2^2 \\
&= \frac{2E}{LC} \xi(x) - \frac{2}{LCR_y} \left(L\psi(x) - \frac{L}{C} \xi^2(x) \right) \\
&= \frac{2E}{LC} \xi(x) - \frac{2}{CR_y} \psi(x) + \frac{2}{C^2 R_y} \xi^2(x).
\end{aligned}
\tag{12}
$$

So, considering $\xi(x) = 0$, the zero dynamics $\dot{\psi}(x) = \eta\big(0, \psi(x)\big)$ is given by:

$$
\eta\big(0, \psi(x)\big) = -\frac{2}{CR_y} \psi(x).
\tag{13}
$$

From (13) it is clear that the zero dynamics is asymptotically stable. Now, it is possible to control i_{LED} by using the output function $y = h(x) = i_L$, finding a relation between these two variables.

2) CONTROL LAW DESIGN FOR LED-DRIVER
By applying the coordinate transformation $z = \Phi(x)$, the nonlinear system (5) becomes a partial linear system. Then, substituting (9) into (8), the following feedback control law is obtained:

$$
u = 1 - \frac{E + Lv}{x_2}, \quad \text{with: } v = -k_p e_L - k_i \int_0^t e_L dt,
\tag{14}
$$

where v is the proposed linear controller, and $e_L = x_1 - i_L^*$ is the output error. The desired reference of the inductor current value is expressed as i_L^*. k_p and k_i are two positive constant gains to be tuning in order to have a desired closed-loop dynamics. Now, by considering $v_c = v_{LED}$, the relation (4) and (1) are used to define the desired LED current i_{LED}^* as a function of the desired inductor current i_L^*, as follows:

$$
i_L^* = \frac{(R_y i_{LED}^* + E_y)^2 - (R_y i_{LED}^* + E_y) E_y}{E R_y}.
\tag{15}
$$

For the implementation of the control law (14) it is necessary to measure both states x_1 and x_2. Note that the term E_y / CR_y is not considered in the input-output linearization design but it is compensated by the control law (14) by using (15).

IV. ACTUATOR FAULT TOLERANT CONTROL SYSTEM
An actuator fault can be modelled as an additive external signal: $u_f = u + f$, where $f = -\theta u$ means the actuator fault affecting the system and θ is the actuator Loss of Effectiveness (LoE). This partial fault could be seen as a LoE in the embedded control target by considering that it generates a faulty PWM signal. Also, faults of energy storage components in the power system can be seen as an actuator partial faults [8]. The inductor degradation can occur due to aging, magnetization, and magnetic conductivity, and the capactance degrades by aging. In this paper, the fault signal is assumed to be constant over time or at least slowly varying, such that $\dot{f} = 0$.

Based on [17] and [18], the following nonlinear observer for actuator fault estimation have been designed. Let consider the nonlinear system (2) and (3), with actuator faults f as an external additive signal and no unmeasurable states x, in the nonlinear adaptive observer form, expressed as:

$$
\dot{x} = \alpha(x, u) + \beta(x, u) f,
\tag{16}
$$

with

$$
\alpha(x, u) = \begin{bmatrix} -\frac{1}{L} x_2 (1 - u) + \frac{1}{L} E \\ \frac{1}{C} x_1 (1 - u) - \frac{1}{CR_y} x_2 + \frac{1}{CR_y} E_y \end{bmatrix},
$$

$$
\beta(x, u) = \begin{bmatrix} \frac{1}{L} x_2 \\ -\frac{1}{C} x_1 \end{bmatrix},
$$

where $\alpha(x, u)$ and $\beta(x, u)$ are two globally Lipschitz functions with respect to x. An adaptive observer can be designed for the system (16) in order to estimate the unknown fault f based on the knowledge of the measurement states x and the input u, as follows:

$$
\begin{aligned}
\dot{\hat{x}} &= \alpha(x, u) + \beta(x, u)\hat{f} - k_z e_x, \\
\dot{\hat{f}} &= -k_f \beta^\top(x, u) e_x^\top,
\end{aligned}
\tag{17}
$$

where $e_x = \hat{x} - x$ is the estimation of state error vector, k_z and k_f are two positive constant gains of the observer. To study the existence of the adaptive observer (17), Proposition 3.1 from [17] can be consulted.

The actuator additive fault estimation signal $\hat{f}$ is used to detect the actuator fault at any time, by comparing it with a constant threshold μ. In a free-fault case, the estimated absolute value $|\hat{f}_i| < \mu$, and close to zero; while in a faulty case the estimated absolute value has a greater value than the threshold, $|\hat{f}_i| \geq \mu$, for indicating a fault occurrence. If the fault estimation value is greater than the threshold then it is considered a faulty case and the alarm indicator is one. The threshold constant value must be established according to experimental results, by reading the fault estimation value in free-fault case and in faulty case. When the actuator LoE is detected and estimated correctly, a new control law is added to the nominal controller to accommodate it.

The fault estimation signal is used with the nominal controller to ensure the tracking trajectory performance of the faulty system to the reference. Hence, the fault accommodation control law is expressed as $\bar{u}_f = u_f - \hat{f}$, where the
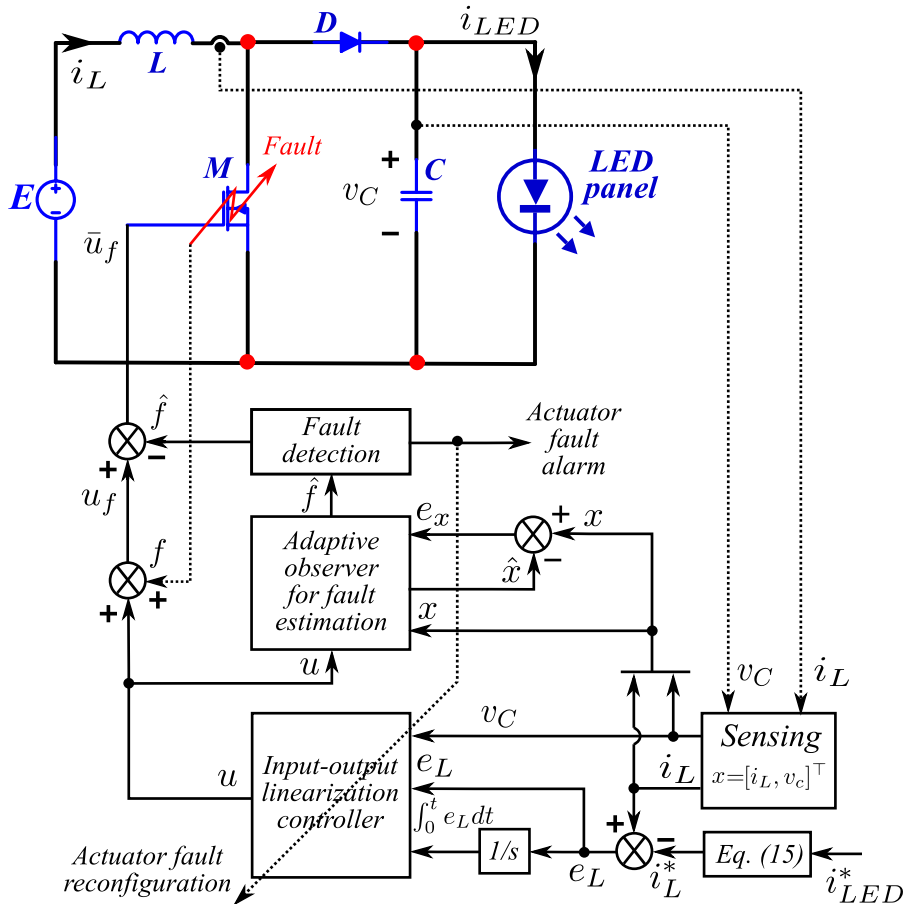
FIGURE 3. FTC scheme applied to LED-driver system.

first part of the equation is the input with actuator fault and the second part is the additive fault estimation to be added in order to accommodate the fault, see Figure 3. This accommodation control law is complemented with a fault reconfiguration strategy to improve the close-loop dynamics, when the fault occurs. If the actuator fault is correctly detected, the input-output linearization controller module uses this information to modify the control parameters k_p and k_i, as shown Figure 3.

V. SIMULATION RESULTS

The LED-driver circuit is simulated using the parameter values given in Section II. Genetic Algorithm (GA) technique is used to search offline the optimal controller gains (14) and observer gains (17), in order to have a desired response of the closed-loop system and fault estimation error subjected to the following cost function equations J_c and J_o, respectively.

Evolutionary algorithms are an important category of machine learning techniques that are based on the evolutionary ideas of natural selection and genetics. A population of individuals, called a generation, compete at a given task with a defined cost function. GA is based on the propagation of generations of individuals by selection through fitness.

Each individual represents a possible solution within a search space. After the initial generation is populated with individuals, each is evaluated and assigned a fitness based on their performance on the cost function metric [19]. In this paper, the Global Optimization Toolbox [20] was used to implement the GA optimization. The performance of the control law (14) and the observer (17) are judged based on the value of the following cost functions:

$$J_c = \min_{e_L, u} \int_0^\infty \left(e_L^\top Q_c e_L + u^\top R_c u \right) dt, \qquad (18)$$

$$J_o = \min_{e_x} \int_0^\infty \left(e_x^\top Q_o e_x \right) dt, \qquad (19)$$

where matrices $Q_c = 1000$ and $Q_o = 1000$ weight the cost deviations of the errors from zero, and $R_c = 0.001$ weight the cost of actuation. The offline procedure for selection of optimal using genetic algorithm technique is shown in Figure 4. The defined parameters for the GA are: a maximum generation of 10 and each generation with population size of 10 individuals, resulting in the following optimal gains: $k_p = 8.4 \times 10^3$, $k_i = 109$, $k_z = 2 \times 10^3$ and $k_f = 4.8$. The obtained reconfiguration control gains are: $k_p = 12.2 \times 10^3$ and $k_i = 250$. For illustrate the performance of the GA algorithm, Figure 5 is presented showing the closed-loop system in
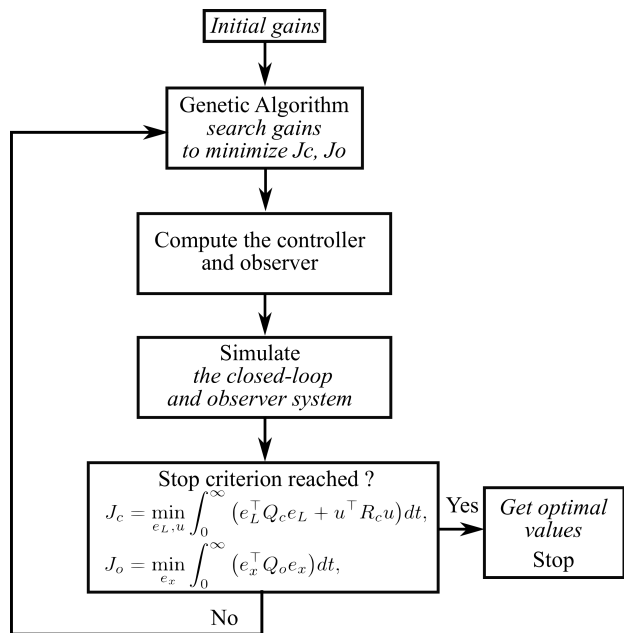
FIGURE 4. Procedure for selection of optimal gains for the controller and observer by using genetic algorithm.
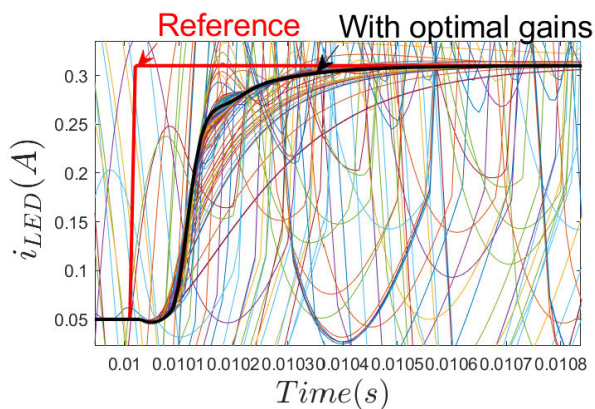

FIGURE 5. Each closed-loop time response to find the optimal control gains.

order to select the optimal gains in (14) by minimizing the cost function (18). Also, this figure shows the application of the procedure for selection of the optimal gains for the controller. Note that the signal with optimal gains (black line) accomplish (18), which is a function with respect to the tracking error and the input authority. Additionally, from Figure 5, clearly some close-loop results are over-damped, under-damped or unstable; consequently they are not the optimal controller gains. Optimal observer gains are calculated using same procedure.

For testing the effectiveness of the proposed scheme, two scenarios were considered, performed in MATLAB/Simulink:

1) SCENARIO 1—FREE-FAULT

Figure 6 shows the reference and the tracking LED current i_{LED} in free-fault case. The reference is a pulse that changes
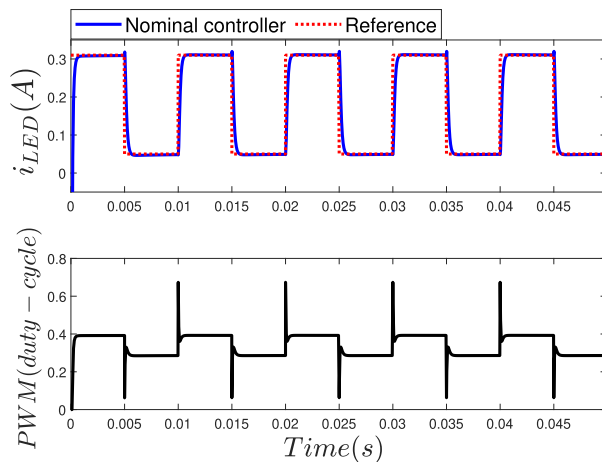

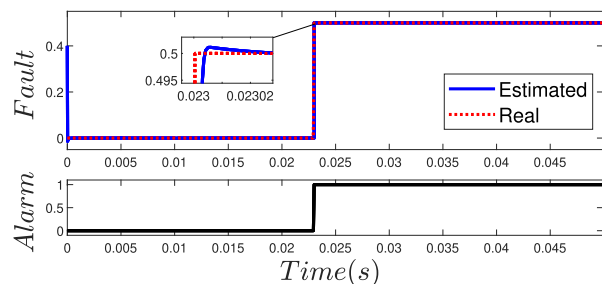**FIGURE 6.** Scenario 1 - LED current tracking and control signal.

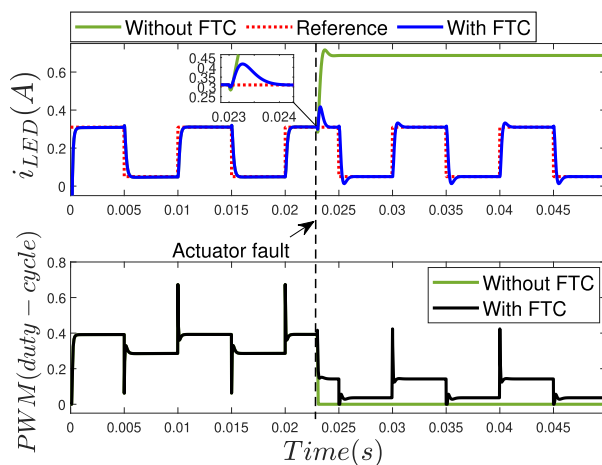**FIGURE 7.** Scenario 2 - Additive fault estimation and alarm indicator.

FIGURE 8. Scenario 2 - LED current comparison between the LED-driver without and with FTC, and control signals.

form $50\,mA$ to $310\,mA$. It is easy to see that the tracking is well performed, which illustrate the effectiveness of the nominal nonlinear controller.

2) SCENARIO 2—CONSTANT PARTIAL FAULT

In this second scenario an additive fault is injected in the actuator with a magnitude of $f = 0.5$ at time 0.023 s, see Figure 7 and 8.

The initial condition of the fault estimation signal $\hat{f}(0) = 0.4$. A smaller error between the real fault and the fault estimation is achieved by using the adaptive nonlinear observer. Additionally, in Figure 8 the LED current comparison between the faulty LED-driver system without and with the FTC strategy using the fault estimation, generated by the adaptive observer, is displayed. The proposed strategy significantly reduces the error between the reference and the LED current. The actuator fault detection is achieved approximately after 17 μs of its occurrence, and consequently the fault accommodation and fault reconfiguration are done to compensate the actuator fault.

VI. CONCLUSION

A nonlinear controller and an actuator FTC system are presented in this paper. The feedback controller is designed using the input-output method while the fault tolerant control is achieved by using a nonlinear adaptive observer for detection, estimation, accommodation and reconfiguration of the fault. The controller and observer gains are tuned using genetic algorithm technique to have a desired closed-loop and fault estimation error response. Two simulation scenarios are performed in order to illustrate the applicability to the LED-driver system. First scenario demonstrates the effectiveness of the feedback controller to track the LED current. Secondly, both the controller and the actuator FTC system are simulated with a fault occurrence to test the fault detection and estimation capabilities of the designed observer. The partial fault is presented as a LoE in the embedded control target or faults in the energy storage components. Fault accommodation and fault reconfiguration are performed by using the fault estimation signal, reducing the fault effect in the closed-loop system. The disadvantage of the proposed strategy is that the gains of the controller and the observer are calculated offline, so it is necessary to have an accurate mathematical model of the LED-driver system.

REFERENCES

[1] X. Liu, S.-X. Guo, Y.-C. Chang, S.-D. Zhu, and S. Wang, "Simple digital PWM and PSM controlled DC–DC boost converter for luminance-regulated WLED driver," *J. China Universities Posts Telecommun.*, vol. 16, no. 2, pp. 98–102, Apr. 2009.

[2] P.-J. Liu and Y.-C. Hsu, "Boost converter with adaptive reference tracking control for dimmable white LED drivers," *Microelectron. J.*, vol. 46, no. 6, pp. 513–518, Jun. 2015.

[3] S. L. Gavini, *Control of Non-Minimum Phase Power Converters*. West Lafayette, IN, USA: Purdue University, 2012.

[4] Y. Zhang and J. Jiang, "Bibliographical review on reconfigurable fault-tolerant control systems," *Annu. Rev. Control*, vol. 32, no. 2, pp. 229–252, 2008.

[5] S.-W. Seo and H. H. Choi, "Digital implementation of fractional order PID-type controller for boost DC–DC converter," *IEEE Access*, vol. 7, pp. 142652–142662, 2019.

[6] L. Cheng, T. Geyer, and S. Manias, "Model predictive control for DC–DC boost converters with reduced-prediction horizon and constant switching frequency," *IEEE Trans. Power Electron.*, vol. 33, no. 10, pp. 9064–9075, Oct. 2018.

[7] G. Li, H. Huang, S. Song, and B. Liu, "A nonlinear control scheme based on input–output-linearized method achieving PFC and robust constant voltage output for boost converters," *Energy Rep.*, vol. 7, pp. 5386–5393, Nov. 2021.

[8] Q. Su, C. Li, X. Guo, X. Zhang, and J. Li, "Robust fault diagnosis for DC–DC boost converters via switched systems," *Control Eng. Pract.*, vol. 112, Jul. 2021, Art. no. 104836.

[9] Z. Liu, Z. Xu, and X. Zhang, "A novel real-time fast fault-tolerance diagnosis and fault adjustment strategy for m-phase interleaved boost converter," *IEEE Access*, vol. 9, pp. 11776–11786, 2021.

[10] L. Xu, R. Ma, R. Xie, J. Xu, Y. Huangfu, and F. Gao, "Open-circuit switch fault diagnosis and fault-tolerant control for output-series interleaved boost DC–DC converter," *IEEE Trans. Transport. Electrific.*, vol. 7, no. 4, pp. 2054–2066, Dec. 2021.

[11] M. W. Ahmad, N. B. Y. Gorla, H. Malik, and S. K. Panda, "A fault diagnosis and postfault reconfiguration scheme for interleaved boost converter in PV-based system," *IEEE Trans. Power Electron.*, vol. 36, no. 4, pp. 3769–3780, Apr. 2021.

[12] E. Pazouki, J. A. De Abreu-Garcia, and Y. Sozer, "A novel fault-tolerant control method for interleaved DC–DC converters under switch fault condition," *IEEE Trans. Ind. Appl.*, vol. 56, no. 1, pp. 519–526, Jan. 2020.

[13] J. L. Soon and D. D.-C. Lu, "Design of fuse–MOSFET pair for fault-tolerant DC/DC converters," *IEEE Trans. Power Electron.*, vol. 31, no. 9, pp. 6069–6074, Sep. 2016.

[14] R. Osorio, J. M. Alonso, N. Vázquez, S. E. Pinto, F. D. J. Sorcia-Vazquez, M. Martinez, and L. M. Barrera, "Fuzzy logic control with an improved algorithm for integrated LED drivers," *IEEE Trans. Ind. Electron.*, vol. 65, no. 9, pp. 6994–7003, Sep. 2018.

[15] A. Isidori, "The zero dynamics of a nonlinear system: From the origin to the latest progresses of a long successful story," *Eur. J. Control*, vol. 19, no. 5, pp. 369–378, Sep. 2013.

[16] S. Bacha, I. Munteanu, and A. I. Bratcu, "Feedback-linearization control applied to power electronic converters," in *Power Electronic Converters Modeling and Control*. Springer, 2014, pp. 307–336.

[17] G. Besançon, "Remarks on nonlinear adaptive observer design," *Syst. Control Lett.*, vol. 41, no. 4, pp. 271–280, Nov. 2000.

[18] G. Ortiz-Torres, P. Castillo, F. D. J. Sorcia-Vazquez, J. Y. Rumbo-Morales, J. A. Brizuela-Mendoza, J. De La Cruz-Soto, and M. Martínez-García, "Fault estimation and fault tolerant control strategies applied to VTOL aerial vehicles with soft and aggressive actuator faults," *IEEE Access*, vol. 8, pp. 10649–10661, 2020.

[19] T. Duriez, S. L. Brunton, and B. R. Noack, *Machine Learning Control-Taming Nonlinear Dynamics and Turbulence*, vol. 116. Springer, 2017.

[20] *Global Optimization Toolbox User's Manual*, MathWorks, Natick, MA, USA, 2014.

GERARDO ORTIZ TORRES (Member, IEEE) received the M.Sc. and Ph.D. degrees in electronic engineering from the National Research and Technological Development Center (CENIDET), in 2014 and 2018, respectively. He is currently a Professor and a Researcher with the Centro Universitario de los Valles, University of Guadalajara. His research interests include fault diagnosis and fault tolerant control systems with applications in unmanned vehicles and process engineering.

JESSE Y. RUMBO-MORALES (Member, IEEE) received the Ph.D. degree from the Centro Nacional de Investigación y Desarrollo Tecnológico (CENIDET). He is currently a full time Professor with the Centro Universitario de los Valles, Universidad de Guadalajara. He has published articles in national and international journals, with cites from Scopus. He has graduated 15 bachelor's degree thesis and 15 technical level thesis. He has participated in projects, particularly in the construction of a prototype pressure swing adsorption to produce bioethanol. He is a member of SNI. His research interests include process control, renewable energy, identification of non-linear systems, and automation.

RENÉ OSORIO SÁNCHEZ was born in Veracruz, Mexico, in 1977. He received the B.Sc. degree in electrical engineering from the Universidad Autónoma de Campeche, Campeche, Mexico, in 1999, and the M.Sc. and Ph.D. degrees in electronics engineering from the Centro Nacional de Investigación y Desarrollo Tecnologico, Cuernavaca, Mexico, in 2001 and 2007, respectively. In June 2009, he was a Researcher with the Instituto Tecnológico de Celaya, Celaya, Mexico. He is currently with the University of Guadalajara, Mexico. He has published about 20 papers in magazines, journals, and international conferences in power electronics.

MARCO ANTONIO RODRÍGUEZ BLANCO received the B.Sc. degree in electronics engineering from the Technological Institute of Orizaba, Veracruz, Mexico, in 1997, and the M.Sc. and Ph.D. degrees in electronics engineering from the National Center for Research and Technological Development (CENIDET), Morelos, Mexico, in 2001 and 2009, respectively. Since 2001, he has been a full-time Professor with the Department of Electronics and Mechatronics Engineering, Autonomous University of Carmen City (UNACAR), Campeche, Mexico. His research interests include power electronics circuit systems, characterization and parameters extraction of power semiconductor devices, and fault detection in motor drives. He is a member of National Research System, Mexico.

• • •

MARIO MARTÍNEZ-GARCÍA received the academic training in computer engineering, in 2001, the master's degree in information technology from the University of Guadalajara, Mexico, in 2005, and the doctorate degree in research and educational innovation from the University of Malaga, Spain, in 2012. He has experience in software development, expert systems, applications for mobile devices, with special interest in research on information technologies applied to education, distributed computing, embedded software, and alternative renewable energy systems.